Analytical Methods

Accepted Manuscript

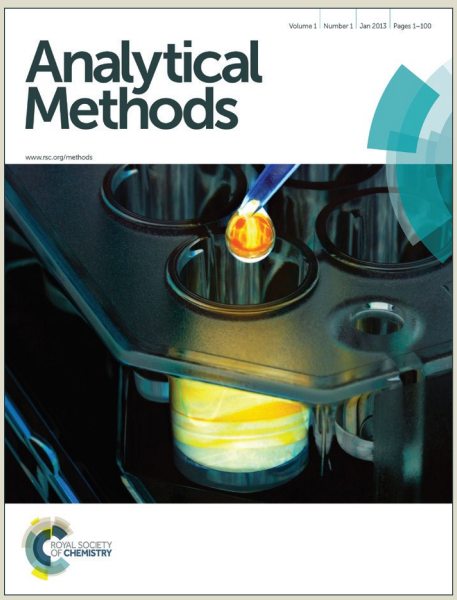

This is an *Accepted Manuscript*, which has been through the Royal Society of Chemistry peer review process and has been accepted for publication.

Accepted Manuscripts are published online shortly after acceptance, before technical editing, formatting and proof reading. Using this free service, authors can make their results available to the community, in citable form, before we publish the edited article. We will replace this *Accepted Manuscript* with the edited and formatted *Advance Article* as soon as it is available.

You can find more information about *Accepted Manuscripts* in the Information for Authors.

Please note that technical editing may introduce minor changes to the text and/or graphics, which may alter content. The journal's standard Terms & Conditions and the Ethical guidelines still apply. In no event shall the Royal Society of Chemistry be held responsible for any errors or omissions in this *Accepted Manuscript* or any consequences arising from the use of any information it contains.

ROYAL SOCIETY OF CHEMISTRY

www.rsc.org/methods

Analysis of phospholipids in *Schizochytrium* sp. S31 by using UPLC-Q-TOF-MS

Leilei Li, Ming Chang, Guanjun Tao, Xiaosan Wang, Yuan Liu, Ruijie Liu*, Qingzhe Jin, Xingguo Wang

State Key Laboratory of Food Science and Technology, Synergetic Innovation Center of Food Safety and Nutrition, School of Food Science and Technology, Jiangnan University, Wuxi 214122, China

Abstract

Phospholipids are the main constituent of cell membranes and play multiple roles in cells for providing the permeability barrier, the supporting matrix, surface of many catalytic processes, precursors of signal processing and macro molecular synthesis. To analyze the composition of the phospholipids from *Schizochytrium* sp. S31, hydrophilic interaction (HILIC) Ultra performance liquid chromatography (UPLC) coupled with quadrupole time of flight (Q-TOF) mass spectrometry (MS) was performed. Finally, phosphatidyl-cholines, -ethanolamines, -inositoles, -glycerol and phosphatidic acid were separated using an acetonitrile/ammonium formate gradient mobile phase. Structural characterizations of 70 phospholipids were identified by LC-MS/MS measurements in negative ion mode. As the major phospholipid in *Schizochytrium* sp. S31, phosphatidylcholine reached 49.8% of total phospholipids and the major phospholipids fatty acids were C16:0 and DHA.

Keywords: Phospholipids; Fatty acids; UPLC-MS; HILIC; *Schizochytrium* sp.

Abbreviations

ATCC	American Type Culture Collection
DHA	Docosahexaenoic acid (22:6)
DPA	Docosapentaenoic acid(22:5)
EIC	Extract ion chromatographic traces

* *Corresponding author: Ruijie Liu, Telephone: +86 510-85876799*

E-mail address: liuruijie163@163.com

ELSD	Evaporative light scattering detector
ESI-MS	Electrospray ionization-mass spectrometry
HILIC	Hydrophilic interaction liquid chromatography
HPLC	High performance liquid chromatography
LOD	Limit of quantity
MS	Mass spectrometry
NI	Negative-ion
NPLC	Normal phase liquid chromatography
PL	Phospholipids
PtdCho	Phosphatidylcholine
PtdEtn	Phosphatidylethanolamine
PtdGro	Phosphatidylglycerol
PtdIns	Phosphatidylinositol
PtdSer	Phosphatidylserine
PtdOH	Phosphatidic acid
PUFA	Polyunsaturated fatty acid(s)
Q-TOF	Quadrupole-time of flight
RPLC	Reversed phase liquid chromatography
RT	Retention time
TIC	Total ion chromatogram
TLC	Thin-layer chromatography
UPLC	Ultra-performance liquid chromatography
UV	Ultraviolet

1. Introduction

Schizochytrium sp. is heterotrophic eukaryotic organisms to produce long chain polyunsaturated fatty acids (PUFAs) [1] . The two main major PUFAs were docosahexaenoic acid (DHA) and docosapentaenoic acid (DPA), accounting for 30-40% of the total fatty acids in the organisms [2]. Previous reports were generally focused on the optimization of fermentation conditions, such as carbon sources [3], phosphate

concentration [4], temperature [5] and oxygen transfer coefficient [6] to improve the production yield of DHA. However, the composition of phospholipids in *Schizochytrium* sp. has not been well documented.

Phospholipids are the main constituents of biological membranes [7]. According to their polar phosphoryl head groups, the phospholipids were mainly divided into six classes: phosphatidylcholine (PtdCho), phosphatidylethanolamine (PtdEtn), phosphatidylserine (PtdSer), phosphatidylinositol (PtdIns), phosphatidylglycerol (PtdGro) and Phosphatidic acid (PtdOH) [8]. Based on the difference of fatty acyl chains, each phospholipid class consists of numerous different structure molecules. Structural variety of phospholipids affects the permeability and fluidity of cell membranes [9]. Phospholipids are not only the main component of the biological membranes, but also involved in some important metabolic activities. A number of studies have suggested that the cell performance could be influenced by PUFA of phospholipids, and low temperature could change the distribution of PUFA in phospholipids [10]. As we known, *Schizochytrium* cells consist of structure lipids (membrane lipid, such as PL) and storage lipids (mainly being neutral lipids). Changes of the head group, glycerol backbone, phospholipid subclass, or stereospecificity will impact the biological activity of the molecule obviously. Furthermore, it is great interesting that the fatty acids composition of each lipid fractions influence the membrane properties and reflect the specificity of intracellular hydrolytic enzymes (i.e. lipases) during synthesis and metabolism of phospholipids. Some researchers investigated the lipids composition in *Schizochytrium* sp. and found that the levels of phospholipids were associated with the DHA content in the cells during the turnover stage [11, 12]. Therefore, the characterization of the phospholipids profile is very necessary for the description of biological function of *Schizochytrium* sp..

Previously, the phospholipids in biological samples were separated through thin-layer chromatography (TLC) [13, 14], which is time-consuming and poorly reproducible. High-performance liquid chromatography (HPLC) coupled with an ultraviolet (UV) or evaporative light scattering (ELSD) detector have been developed

to separate the different phospholipid classes [15, 16]. However, these methods still have some limitations, such as poor selectivity and sensitivity. Recently, researchers have developed different approaches for quantifying phospholipids by high performance liquid chromatography-mass spectrometry (HPLC-MS) [17, 18]. Recently, mass spectrometry (MS) has been widely used in the analysis of various compounds because of the high selectivity and sensitivity. HPLC-MS separation of phospholipids classes have been reported using either normal phase liquid chromatography (NPLC) or reversed phase liquid chromatography (RPLC). The different species of phospholipids were separated by NPLC-MS and RPLC-MS based on their polar groups and the length and saturation degrees of their fatty acid chain, respectively [19]. However, nonpolar solvents (hexane), chloroform or isooctane were usually used as mobile phases which were not compatible with MS analysis for NPLC. In addition, the class separation of different phospholipid classes was not satisfied with RPLC.

Hydrophilic Interaction Liquid Chromatography (HILIC) was first introduced by Alpert in 1990 [20]. The combination of normal- and reversed-phase chromatography is a suitable tool for the separation of phospholipid classes and has excellent resolution for different classes of polar solutes. Several studies have characterized the phospholipids using HILIC [21-23]. Compared with NPLC, HILIC is more suitable for on-line electrospray ionization-mass spectrometry (ESI-MS) detection, because its eluting solvents are ESI-compatible, and with RPLC, HILIC produce a great resolution for the phospholipids separation[24, 25]. Above all, a HILIC coupled to ESI-MS/MS analysis method was developed to construct the phospholipids profile and investigate the relationship between phospholipids and the content of PUFAs of *Schizochytrium* sp.

2. Materials and Methods

2.1 Materials

Phospholipids standards, 1, 2-dimyristoyl-*sn*-Glycero-3-Phosphocholine, 1, 2-Dimyristoyl-*sn*-Glycero-3-Phosphoethanolamine, 1, 2-Dipalmisoyl-*sn*-Glycero-3-Phosphoinositol (Ammonium Salt) were purchased from

Avanti Polar Lipids (Alabaster, AL, USA). 3-*sn*-phosphatidic acid sodium salt and 1-(3-*sn*-phosphatidyl)-rac-glycerol sodium salt were obtained from Sigma-Aldrich (USA). Methanol (LC−MS grade), acetonitrile (LC−MS grade) and chloroform (HPLC grade) were provided with TEDIA (Tedia Company Inc, Ohio, USA).

2.2 Microorganism and Shake flask cultures

Schizochytrium strains were obtained from the American Type Culture Collection (ATCC, Manassas, VA). The inoculum medium consisted of (g/L): glucose, 30; yeast extract, 5; NaCl, 0.3; Na_2SO_4, 15; sodium glutamate, 5; K_2SO_4, 1; $MgSO_4 \cdot 7H_2O$, 3; K_2HPO_4, 2; KH_2PO_4, 3; $CaCl_2$, 0.02; vitamin B_1, 0.005; vitamin B_6, 0.002; vitamin B_{12}, 0.005. The fermentation medium comprised the basal ingredients (g/L): glucose, 100; yeast extract, 10; NaCl, 0.3; Na_2SO_4, 15; sodium glutamate, 15; K_2SO_4, 1; $MgSO_4 \cdot 7H_2O$, 4; KH_2PO_4, 0.1; $CaCl_2$, 0.05; vitamin B_1, 0.008; vitamin B_6, 0.002; vitamin B_{12}, 0.008. Its pH was adjusted to 6.5-7.0 before it was autoclaved at 114℃ for 20 min. The inoculum medium were inoculated with 10% (v/v) of exponentially growing inoculum and incubated at 25℃ in an orbital shaker at a 250 rpm. The cells were grown under aerobic conditions (50 mL of fluid nutrient medium in 250-mL flasks), and then harvested at the early stationary phase by centrifugation at 4000×g for 10 min followed by freeze-drying.

2.3. Extraction of the lipid fraction of the samples

The lipid fraction was extracted from 0.1 g of the *Schizochytrium* sp. S31 samples, according to the Bligh and Dyer method [26]. Briefly, each 0.1 g sample was added a mixture of 3 ml methanol, 1.5 ml chloroform and 1.2 ml distilled water. After vortex for 3 minutes and ultrasonic for 30 minutes, 1.5 ml chloroform was added into the mixture. Then 1.5 ml distilled water was added and ultrasonic continued for another 30 minutes. The mixture was centrifuged at 4,000 rpm for 10 min and the lipid phase at the low layer was isolated, evaporated under nitrogen. The final dried lipid extracts were re-dissolved in 1 mL of chloroform/methanol 2:1 (v/v) prior to analysis.

2.4. Ultra-performance liquid chromatography Mass Spectrometry

The Ultra-performance Liquid Chromatography (UPLC) system (Waters, Milford, Massachusetts, USA) was equipped with BEH HILIC column (100 × 1 mm i. d., 1.7

μm particle size). Mobile phase A was acetonitrile. Mobile phase B was 50 mM ammonium acetate containing 0.1% formic acid (pH=3.65). The binary gradient started with 5% B for 4 min, then changed 40% B within 10 min and held for 5 min. The flow rate was 300 μl/min. The column and sample room temperatures were 40 ℃ and 4 °C, respectively. After each analysis, the column was flushed for 5 min with 5% of B before the next analysis was started.

A quadrupole time-of-flight (Q-TOF) mass spectrometry (MS) instrument (Waters, Milford, Massachusetts, USA) was used to identify and quantify the phospholipids in samples. Negative-ion (-ve) mode was used at an optimized condition as follows: capillary voltage, 3.0 kV; cone voltage, 30 V; source temperature, 100°C; desolvation temperature, 400 °C; collision gas, argon; desolvation gas (nitrogen) flow rate, 700 L/h. Data were collected between *m/z* 50 and 1500 Da with a scan duration of 0.2 s. The MS/MS experiments were performed using different collision energy for each compound, which was presented in Table 1. Instrument control and data analysis were performed using the MassLynx 4.1 software (Waters.).

2.5. Quantitative analysis

The concentration of each phospholipid was calculated using its calibration curve built with known concentrations of corresponding standards. All data analyzed were corrected for 13C isotope effects as described by Han et al [27].

3. Results

3.1. Separation of phospholipids using UPLC

In this study, the separation of five phospholipid standards was achieved within 20 min. As shown in Fig. 1A, the first eluted component was PtdGro, followed by PtdIns, PtdEtn, PtdOH and PtdCho. The separation trend of phospholipids on a BEH column in HILIC mode relies on negative charge lipids and neutral lipids respectively. The separation of the negative charge phospholipids was based on the combined effect of electrostatic interactions and hydrophilic interaction. The elution of phospholipids depends on the polarity of the compounds: the less polar the lipid was, the shorter the

retention was. Although there was a slight overlap between PtdEtn and PtdOH, the classes of phospholipids were separated from each other completely when monitored by the mass spectrometry.

The Total Ion Chromatogram (TIC) of the phospholipid extracts is showed in Fig. 1B. The PL classes from *Schizochytrium* sp. S31 were well separated from each other as the above described UPLC-MS conditions. Within the first 4 min, the larger amounts of nonpolar compounds were eluted and followed by most of the phospholipids between 4 and 10 min. The elution order for each compound was as same as the phospholipid standard mixture. Because different phospholipid molecular species within a class have the same polar head, their chromatographic retention in HILIC is very similar. The differences in retention times for the compounds within one class are less than those from two different classes. The different phospholipid molecular species were successfully identified by MS.

Fig. 2 shows the Extract Ion Chromatographic (EIC) traces of $[M-H]^-$ ions of 1,2-didocosahexaenoyl-*sn*-glycero-3-phosphoethanolamine (22:6/22:6-PtdEtn) and 1-palmitoyl-2-docosahexaenoyl-*sn*-glycero-3-phosphoethanolamine (16:0/22:6-PtdEtn) with retention time (RT) of 7.35 min and 7.46 min, respectively, as well as $[M+HCOOH]^-$ ions of 1-palmitoyl-2-docosahexaenoyl-*sn*-glycero-3-phosphocholine (16:0/22:6-PtdCho) and 1-palmitoyl-2-docosahexaenoyl-*sn*-glycero-3-phosphocholine (14:0/22:6-PtdCho) which eluted at retention time of 8.25 min and 8.38 min, respectively. These species contained different fatty acids connected to phosphatide backbone. The elution order of these species depended upon the chain length of fatty acid as well as the saturation degree. In general, the elution order within the same PL class follows the rule: the retention time decreases with increasing fatty acid chain length, while the retention time decreases with increasing the saturation degree of the same chain length of fatty acid [19].

3.2. Determination of different phospholipid classes by mass spectrometry.

The molecular ion peaks from the different phospholipid classes were detected by negative ion full-scan ESI-MS analysis (Fig.3). The major classes of phospholipids

possess a net negative charge at neutral pH. Accordingly, these phospholipids can be effectively distinguished as $[M-H]^-$ as the molecular ion peak in the negative ion mode (such as PtdGro, PtdOH, PtdIns, PtdEtn) based on the nitrogen rule. In the negative ion mode, PtdEtn (with one nitrogen atom) showed signals at even numbers *m/z* values, whereas PtdGro, PtdOH, PtdIns (without nitrogen atom) show signals of uneven numbers *m/z* values. The other classes, such as PtdCho, having phosphocholine as the polar head, were determined by formatting adducts $[M + HCOO]^-$.

In order to determine the different phospholipid species within the same class, tandem mass spectrum was investigated. The fragmentations created from the compound were compared with those obtained from known standards and previous data.

3.3. Determination of phospholipid molecular species by MS/MS fragmentation.

A typical identification of one molecular species of PtdOH is presented here in detail. Electrospray ionization mass spectra of PtdOH from the extracts of *Schizochytrium* sp. S31 displayed multiple individual molecular species in the indicated proportions (Fig. 3B and Table 2).The predominant molecular species (*m/z* 719.5) of PtdOH in *Schizochytrium* sp. S31 contains C16:0 and DHA at a different position. The obtained MS^2 spectra of PtdOH species was illustrated in Fig.4B. The carboxylate anion fragment ions at *m/z* 255.5 (16:0) and *m/z* 327.5 (22:6) were detected. Fragment ion of *m/z* 409.2 and 391.2 corresponded to 16:0 lyso-PtdOH with the loss of neutral fatty acid or ketone from the *sn*-2 position. The information on the distribution of FA among the *sn* positions by the fragmentations discussed above was not clear due to the abundance ratio of the carboxylate anions was associated with many factors, such as phospholipid class and collision energy [28]. In this assay, the phospholipids isolated from alga mostly contained a saturated fatty acid at the *sn*-1 position and an unsaturated fatty acid at the *sn*-2 position [29]. Therefore, *m/z* 719.5 was labeled as 16:0/22:6 PtdOH molecular species.

The other three phospholipids classes, such as PtdEtn/PtdIns/PtdGro, have similar fragmentation behavior as PtdOH with both $[M-H]^-$ ions in negative ESI mode.

The product ion $[C_3H_6O_5P]^-$ (*m/z*153) was also discovered and was a general and common fragment generated by all the glycerophospholipids, and it is higher in PtdOH, PtdIns and PtdGro, but lower in PtdCho and PtdEtn. It was used to detect all the glycerophospholipids that could form negative ions. Besides, the determination of these lipid classes by MS/MS based on specific fragments have been reported in the previous studies [30, 31].

Concerning PtdCho (Fig. 4C), tandem MS on $[M-H]^-$ ions failed to provide an apparent information on the acyl chain. The predominant product ion was formed through formate adducts and shown in Figure 4C. In this case, the main product ion $[M-15]^-$ in the MS^2 spectrum was contributed by the loss of CH_3 from the choline group. Furthermore, the information provided on the fatty acid substituents was able to identify the phospholipid species. The peaks at *m/z* 327.5 and 255.5 corresponded to $[C_{15}H_{31}COO]^-$ and $[C_{21}H_{31}COO]^-$, respectively. The profile of the mass spectrum demonstrated that this compound was C16:0/C22:6-PtdCho.

3.4. Method Validation

The developed method was validated in terms of accuracy, linearity, %RSD, recovery, limit of quantitation (LOQ) and the relevant analytical parameters for quantitative analysis of the target compounds (Table 3). To be more specific, linearity was studied at five concentrations, ranging from 1.25 to 25 μg/mL. Calibration curves showed coefficients of correlation (R) higher than 0.99 with RSDs below 10%. The LOQ of phospholipids was determined at a signal-to-noise ratio of 10 and showed in Table 3.

In addition, this method was applied to analyze the phospholipids in *Schizochytrium* sp. S31 to confirm the validity of this method, a spiked recovery method was used to evaluate the developed method. The recoveries of the five standards are between 94 and 120 % in Table 3.

4. Discussion

4.1. Separation of phospholipids using UPLC

Although HPLC-MS separation of PL in algae was reported in several papers, some of them had controversial results or different elution order of individual phospholipids

classes. Yan Xiaojun[31] used UPLC-ESI-Q-TOF-MS to directly analyze the total lipid extracts from the microalga *Nitzschia closterium*. The RPLC separation, performed on a C^8 Column, identified only 18 phospholipid molecular species. Using a silica gel column and chloroform/acetone mobile phase system, Astrid Vieler [32] separated the lipid extracts from the unicellular green alga *Chlamydomonas reinhardtii* and the diatom *Cyclotella meneghiniana* and found three phospholipid classes. All the methods mentioned above failed to give a comprehensive chemical characterization of the phospholipids.

RPLC and NPLC systems have been reported in separations both between PL classes and within PL class. Still, they have limitations for separation of PLs. With NPLC, when it coupled to mass detector, the solvent it used was not compatible. With RPLC, different compounds within the various PL classes were separated successfully but between-class separation was not obtained completely. As the result, ion suppression of lipids of a certain class can occur due to the presence of lipids of another class. Therefore, the aim of the current study was to develop a separation method which could provide better class separation. As for HILIC, it can separate the phospholipids classes successfully, and more suitable for MS analysis.

In our study, a gradient HILIC method using a BEH column was developed for separating PL classes with adding 50 m mol/L ammonium formate to the mobile phase for increasing the separation resolution and selectivity. The results showed that the peak shape and chromatographic behavior of PL were influenced by the addition of ammonium formate greatly. After the optimization of separation conditions such as its concentration and pH of the mobile phase, phospholipids classes present in the *Schizochytrium* sp. S31 was well separated (Fig.1)

4.2. Phospholipid profiles of *Schizochytrium* sp. S31

The fermentation time was chosen at the 1st day in order to guarantee the highest incorporation of PL in *Schizochytrium* sp. S31 lipids. The identified molecular species composition of each phospholipid class in *Schizochytrium* sp. S31 were shown in Table 3. For *Schizochytrium* sp. S31, PtdCho was the major phospholipid, making up 49.8% of all quantified phospholipids. In other species of *Schizochytrium*, PtdCho

was also accounted for the largest proportion of PL. It was similar to *Schizochytrium* sp. S31, in which the proportions varied widely among different species. King waifan [33] studied the lipid class composition and fatty acid composition of different lipid fractions of *Schizochytrium mangrovei* FB3 and concluded that PtdCho was the major polar lipid and PLs contained a higher DHA percentage in total fatty acids. Guang wang [34] reported that in *schizochytrium* cells, PtdCho was also the essential components and made up 35.4% of the total phospholipids. The high content of PtdCho in *Schizochytrium* sp. can also be illustrated in the study of E. Morita [35] in which PtdCho were identified in *Schizochytrium* SR21. The authors identified that PtdCho as the main phospholipid class constituted 14.4±2.5% of the total lipids in the 4-h cultured cells. PtdCho is the most abundant lipid constituent of the membranes of most eukaryotes including yeast. A significant function of PtdCho is to develop a stable matrix for (intra) cellular membranes, which is promoted by its geometrical shape and physico-chemical properties. It also shapes the lateral pressure profile within membranes with other membrane components. Another special function of PtdCho is to act as a reservoir of lipid messengers. Many signaling cascades involve a step in which PtdCho is hydrolyzed to yield PtdOH, lyso-PtdCho and/or free fatty acids [36]. PtdIns was the second most abundant phospholipid, which accounted for 26.9% of the phospholipids. As well as PtdCho, PtdIns is a bilayer forming phospholipid that compensates for the replacement of PtdCho that forms somewhat less stable bilayers [37]. Several studies shown that the phosphatidylinositol response has been implicated in membrane signaling and cell activation [38, 39]. Besides PtdCho and PtdIns, PtdOH and PtdEtn were equally abundant and in a range from 8.2% to 13.1% of PL. PtdGro was also detected in *Schizochytrium* sp. S31, but their amounts were relatively low as compared to other PLs.

Biological membranes were not only various in the PL classes, but also in their fatty acid composition. Different phospholipid with various fatty acids have been identified in the lipidome of cellular membranes. Each fatty acid has its own unique properties, indicating that they constitute the bulk of the membrane lipid matrix, but as well as influencing generic physical properties of the membrane. As Table 3 shown,

the phospholipid of *Schizochytrium* sp. S31 was composed primarily of C16:0 and DHA. In fact, PLs are the essential components of cell membranes. The higher degree of unsaturation of their PLs is related to the membrane fluidity and important to the cell normal functions. Results from Lu-Jing Ren[12] demonstrated that the percentage of unsaturated fatty acids, DHA and EPA in PL fraction was higher than that in neutral lipids fraction. The study by Eriko Abe [40]also reported that in phospholipids of *Schizochytrium* sp. F26-b, DHA was found to make up about 50% of the total fatty acid.

After the investigation of individual classes of phospholipids, all phospholipids except PtdGro were found to contain DHA as the predominant fatty acid while saturated fatty acids such as C16:0 were predominant in the PtdGro fraction (Table 3). This results were in consistence with the earlier reports [34]. PtdGro had much less total polyunsaturated fatty acids and more total saturated fatty acids than that in PtdCho or PtdEtn. As it is still difficult to explain why DHA content in the PtdGro is lower than other PL, this should be focused on in the future.

Acknowledgements

This work was supported by "National Natural Science Foundation of China (Grant Nos. 31401619)" and "The Natural Science Foundation of Jiangsu Province (BK20140156)".

References

1. J. C. Lippmeier, K. Crawford, C. Owen, A. Rivas, J. Metz and K. Apt, *Lipids*, 2009, **44**, 621-630.
2. L. Qu, L. J. Ren, G. N. Sun, X. J. Ji, Z. K. Nie and H. Huang, *Bioprocess and biosystems engineering*, 2013, **36**, 1905-1912.
3. J. Li, R. Liu, G. Chang, X. Li, M. Chang, Y. Liu, Q. Jin and X. Wang, *Bioresource technology*, 2015, **177**, 51-57.
4. L. J. Ren, Y. Feng, J. Li, L. Qu and H. Huang, *Bioprocess and biosystems engineering*, 2013, **36**, 1177-1183.
5. Y. Zeng, X. J. Ji, M. Lian, L. J. Ren, L. J. Jin, P. K. Ouyang and H. Huang, *Applied biochemistry and biotechnology*, 2011, **164**, 249-255.
6. G. Chang, N. Gao, G. Tian, Q. Wu, M. Chang and X. Wang, *Bioresource technology*, 2013,

142, 400-406.
7. G. van Meer, D. R. Voelker and G. W. Feigenson, *Nature reviews. Molecular cell biology*, 2008, **9**, 112-124.
8. M. Hermansson, K. Hokynar and P. Somerharju, *Progress in Lipid Research*, 2011, **50**, 240-257.
9. M. F. Quartacci, E. Cosi and F. Navari‐Izzo, *Journal of Experimental Botany*, 2001, **52**, 77-84.
10. G.-Q. Chen, Y. Jiang and F. Chen, *Food chemistry*, 2008, **109**, 88-94.
11. H. Okuyama, Y. Orikasa and T. Nishida, *Biotechnology letters*, 2007, **29**, 1977-1981.
12. L. J. Ren, G. N. Sun, X. J. Ji, X. C. Hu and H. Huang, *Bioresource technology*, 2014, **157C**, 107-113.
13. K. Dyńska-Kukulska and W. Ciesielski, *Reviews in Analytical Chemistry*, 2012, **31**.
14. J. Touchstone, J. Chen and K. Beaver, *Lipids*, 1980, **15**, 61-62.
15. G. M. Patton, J. M. Fasulo and S. J. Robins, *Journal of lipid research*, 1982, **23**, 190-196.
16. K. C. N. Terry L. Kaduce, and Arthur A.Spector, *Journal of lipid research*, 1983, **24**, 1398-1403.
17. H.-Y. Kim, T.-C. L. Wang and Y.-C. Ma, *Analytical chemistry*, 1994, **66**, 3977-3982.
18. U. Sommer, H. Herscovitz, F. K. Welty and C. E. Costello, *Journal of lipid research*, 2006, **47**, 804-814.
19. C. Zhu, A. Dane, G. Spijksma, M. Wang, J. van der Greef, G. Luo, T. Hankemeier and R. J. Vreeken, *Journal of chromatography. A*, 2012, **1220**, 26-34.
20. A. J. Alpert, *Journal of Chromatography A*, 1990, **499**, 177-196.
21. P. Donato, F. Cacciola, F. Cichello, M. Russo, P. Dugo and L. Mondello, *Journal of chromatography. A*, 2011, **1218**, 6476-6482.
22. T. Rezanka, L. Siristova, D. Matoulkova and K. Sigler, *Lipids*, 2011, **46**, 765-780.
23. L. Zheng, R. T'Kind, S. Decuypere, S. J. von Freyend, G. H. Coombs and D. G. Watson, *Rapid communications in mass spectrometry : RCM*, 2010, **24**, 2074-2082.
24. B. Tan, A. Negahban, T. McDonald, Y. Zhang and C. Holliman, *Bioanalysis*, 2012, **4**, 2049-2058.
25. L. Zheng, R. T'Kind, S. Decuypere, S. J. von Freyend, G. H. Coombs and D. G. Watson, *Rapid Communications in Mass Spectrometry*, 2010, **24**, 2074-2082.
26. E. G. Bligh and W. J. Dyer, *Canadian Journal of Biochemistry and Physiology*, 1959, **37**, 911-917.
27. X. Han and R. W. Gross, *Mass Spectrometry Reviews*, 2005, **24**, 367-412.
28. E. Hvattum, G. Hagelin and Å. Larsen, *Rapid Communications in Mass Spectrometry*, 1998, **12**, 1405-1409.
29. M. Petković, J. Schiller, M. Müller, S. Benard, S. Reichl, K. Arnold and J. Arnhold, *Analytical Biochemistry*, 2001, **289**, 202-216.
30. I. Losito, R. Patruno, E. Conte, T. R. Cataldi, F. M. Megli and F. Palmisano, *Analytical chemistry*, 2013, **85**, 6405-6413.
31. X. Yan, H. Li, J. Xu and C. Zhou, *Chinese Journal of Oceanology and Limnology*, 2010, **28**, 106-112.
32. A. Vieler, C. Wilhelm, R. Goss, R. Suss and J. Schiller, *Chemistry and physics of lipids*, 2007, **150**, 143-155.

33. K.-W. Fan, Y. Jiang, Y.-W. Faan and F. Chen, *Journal of agricultural and food chemistry*, 2007, **55**, 2906-2910.
34. G. Wang and T. Wang, *Journal of the American Oil Chemists' Society*, 2012, **89**, 135-143.
35. E. Morita, Y. Kumon, T. Nakahara, S. Kagiwada and T. Noguchi, *Marine biotechnology*, 2006, **8**, 319-327.
36. A. I. de Kroon, P. J. Rijken and C. H. De Smet, *Progress in lipid research*, 2013, **52**, 374-394.
37. A. I. P. M. de Kroon, *Biochimica et Biophysica Acta (BBA) - Molecular and Cell Biology of Lipids*, 2007, **1771**, 343-352.
38. S. A. Grupp and J. A. Harmony, *The Journal of Immunology*, 1985, **134**, 4087-4094.
39. L. C. Cantley, *Science*, 2002, **296**, 1655-1657.
40. E. Abe, Y. Hayashi, Y. Hama, M. Hayashi, M. Inagaki and M. Ito, *Journal of biochemistry*, 2006, **140**, 247-253.

Fig. 1. A: UPLC-MS detection of phospholipids standard. The figure shows negative mode detection of C16:0/C18:1n-9 PtdGro (4.84 min), C16:0/C16:0 PtdIns (7.18 min), C14:0/C14:0 PtdEtn (7.61 min), C16:0/C18:1n-9 PtdOH (7.74 min), C14:0/C14:0 PtdCho (8.54 min). B: HILIC/MS-MS chromatogram of the phospholipids from *Schizochytrium* sp. S31

Fig 2. The extract ion chromatographic traces (EIC) of precursor ions of different phospholipid species. A: C22:6/C22:6 PtdEtn (7.35 min), B: C16:0/C22:6 PtdEtn (7.46 min), C: C22:6/C22:6 PtdCho (8.25 min), D: C16:0/C22:6 PtdCho (8.38 min)

Fig.3. ESI-MS spectrum averaged over the band observed for different phospholipids classes in the HILIC-ESI-MS TIC chromatogram shown in Figure 1. A: PtdGro; B: PtdOH; C:PtdCho; D:PtdEtn; E:PtdIns

Fig. 4. MS/MS spectrum of different phospholipids species obtain in the ESI. A: C16:0/C16:0-PtdGro; B: C16:0/C22:6-PtdOH; C: C16:0/C22:6-PtdCho; D: C16:0/C22:6-PtdEtn; E: C16:0/C22:6-PtdIns

Tables:

Table 1. The precursor ions and Collision Energy for different phospholipids classes

class	Precursor ions	Collision Energy (eV)
PtdCho	$[M+HCOOH]^-$	30
PtdEtn	$[M-H]^-$	25
PtdOH	$[M-H]^-$	25
PtdIns	$[M-H]^-$	30
PtdGro	$[M-H]^-$	30

Table 2. Overview of PLs Identified by HILIC−ESI-MS in Lipid Extracts of *Schizochytrium* sp. S31

Class	species	peak(m/z)	concentration（μg/g）	RSD(%)
PtdCho	C14:0/C14:0	722.5	14.10	5.6
	C14:0/C15:0	736.5	2.71	9.3
	C14:0/C16:0	750.5	45.42	2.1
	C15:0/C16:1	762.5	21.63	1.9
	C15:0/C16:0	764.5	4.99	5.3
	C16:0/C16:0	778.5	52.40	3.2
	C14:0/C22:6	822.5	117.98	2.8
	C16:0/C20:5	824.5	40.11	2.5
	C15:0/C22:6	836.5	33.57	3.4
	C15:0/C22:5	838.5	16.11	4.0
	C17:0/C20:4n-6	840.5	39.63	4.0
	C16:0/C22:6	850.5	1573.35	1.6
	C16:0/C22:5	852.5	208.45	5.1
	C18:1n-9/C22:6	876.5	36.23	1.3
	C18:0/C22:6	878.6	19.77	4.2
	C20:5/C22:6	896.5	60.11	6.4
	C20:4n-6/C22:6	898.5	32.09	1.5
	C22:6/C22:6	922.5	1004.38	5.1
	C22:5/C22:6	924.5	226.04	4.5
	C22:0/C22:6	934.6	24.57	7.0
	C22:0/C22:5	936.6	6.67	7.5
PtdEtn	C17:0/C18:2n-6	728.5	5.07	3.5
	C14:0/C22:6	734.5	10.41	8.3
	C15:0/C22:6	748.5	5.47	7.5
	C16:0/C22:6	762.5	269.02	3.4
	C16:0/C22:5	764.5	33.36	3.4

	C17:0/C22:6	776.5	24.09	6.5
	C20:5/C22:6	808.5	27.75	6.7
	C20:4n-6/C22:6	810.5	12.67	6.7
	C20:5/C22:0	820.6	4.63	9.5
	C22:6/C22:6	834.5	156.10	5.2
	C22:5/C22:6	836.5	28.52	5.5
	C22:0/C22:6	846.6	11.30	7.4
	C22:0/C22:5	848.6	3.16	3.5
PtdIns	C14:0/C22:6	853.5	18.78	4.8
	C14:0/C22:5	855.5	8.63	4.5
	C15:0/C22:6	867.5	19.47	5.4
	C15:0/C22:5	869.5	9.01	4.3
	C16:1/C22:6	879.5	8.58	5.5
	C16:0/C22:6	881.5	1205.89	1.8
	C16:0/C22:5	883.5	487.01	2.5
	C17:0/C22:6	895.5	10.33	4.5
	C17:0/C22:5	897.6	3.44	6.5
	C18:1n-9/C22:6	907.5	5.16	9.4
	C18:0/C22:6	909.6	6.12	9.5
	C20:5/C22:0	939.6	57.93	5.0
	C20:4n-6/C22:0	941.6	38.20	6.8
	C22:6/C22:6	953.5	23.01	6.7
	C22:5/C22:6	955.5	11.67	8.4
	C22:0/C22:6	965.6	9.39	4.5
	C22:0/C22:5	967.6	11.49	4.6
PtdGro	C14:0/C16:0	693.5	2.16	7.2
	C15:0/C16:0	707.5	2.69	2.4
	C16:0/C16:0	721.5	95.41	4.1
	C16:0/C17:0	735.5	1.25	5.1

	C16:0/C18:0	749.6	1.52	5.1
	C14:0/C22:6	765.5	1.17	5.4
	C14:0/C22:0	777.6	2.67	3.5
	C15:0/C22:6	779.5	1.27	8.4
	C16:0/C22:6	793.5	20.41	5.1
	C16:0/C22:5	795.5	5.61	7.2
	C20:5/C22:6	839.5	4.88	5.4
	C20:4n-6/C22:6	841.5	1.93	6.4
	C22:6/C22:6	865.5	4.45	7.4
	C22:5/C22:6	867.5	1.70	9.6
PtdOH	C14:0/C22:6	691.5	75.27	5.4
	C16:0/C22:6	719.5	388.11	4.1
	C16:0/C22:5	721.5	129.90	4.3
	C22:6/C22:6	791.5	247.43	5.7
	C22:5/C22:6	793.5	101.57	6.7

406

407

Table 3. The linearity, and recovery of five standards

Compounds	Calibration curves	R^2	RSD(%)	Recovery (%)	LOQ(μg/ml)
PtdCho	y=0.9161x+0.8966	0.9904	4.6	108-112	0.2
PtdEtn	y=3.464.3x+0.0049	0.9952	8.5	96-120	0.15
PtdGro	y=62.634x+2.791	0.9996	5.7	104-109	0.1
PtdOH	y=1.02x-4.6775	0.9999	6.5	94-101	0.25
PtdIns	y=2.46x+0.0032	0.9915	5.9	98-116	5

Figure 1

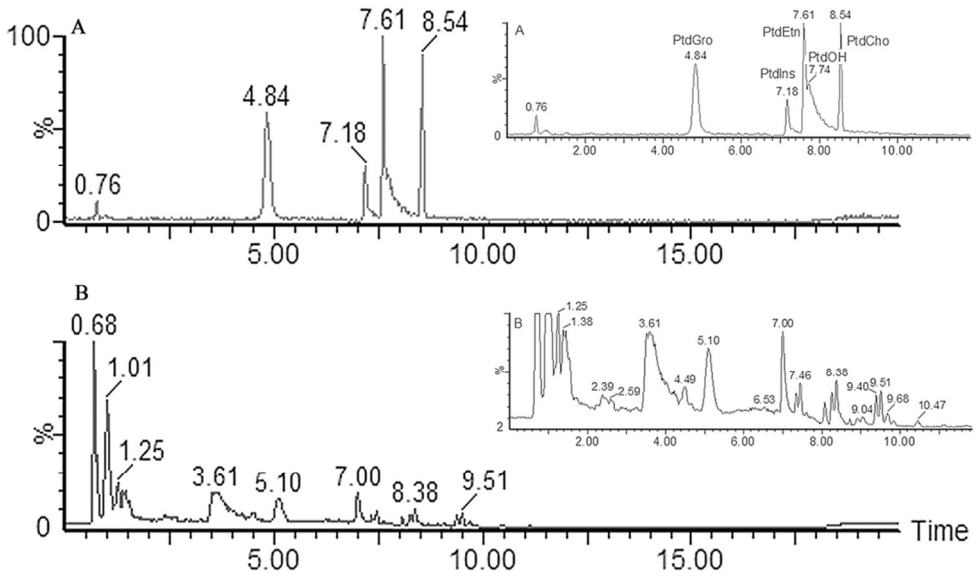

91x56mm (300 x 300 DPI)

Figure 2

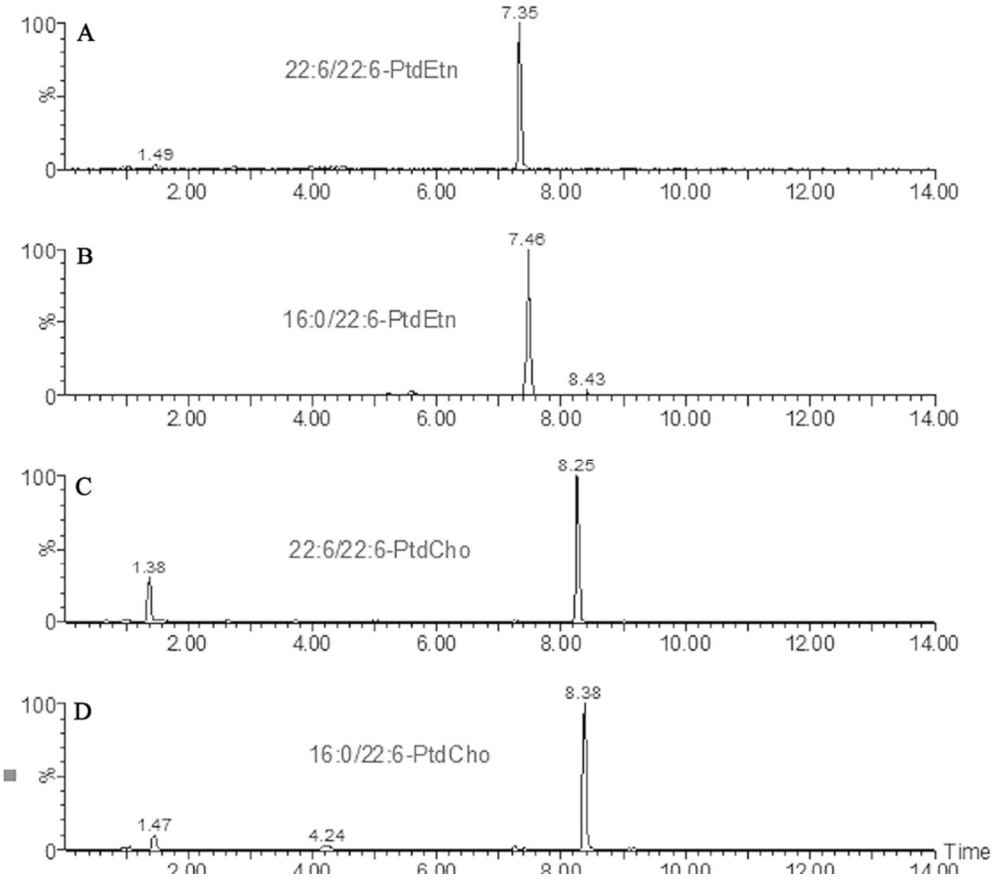

78x73mm (300 x 300 DPI)

Figure 3

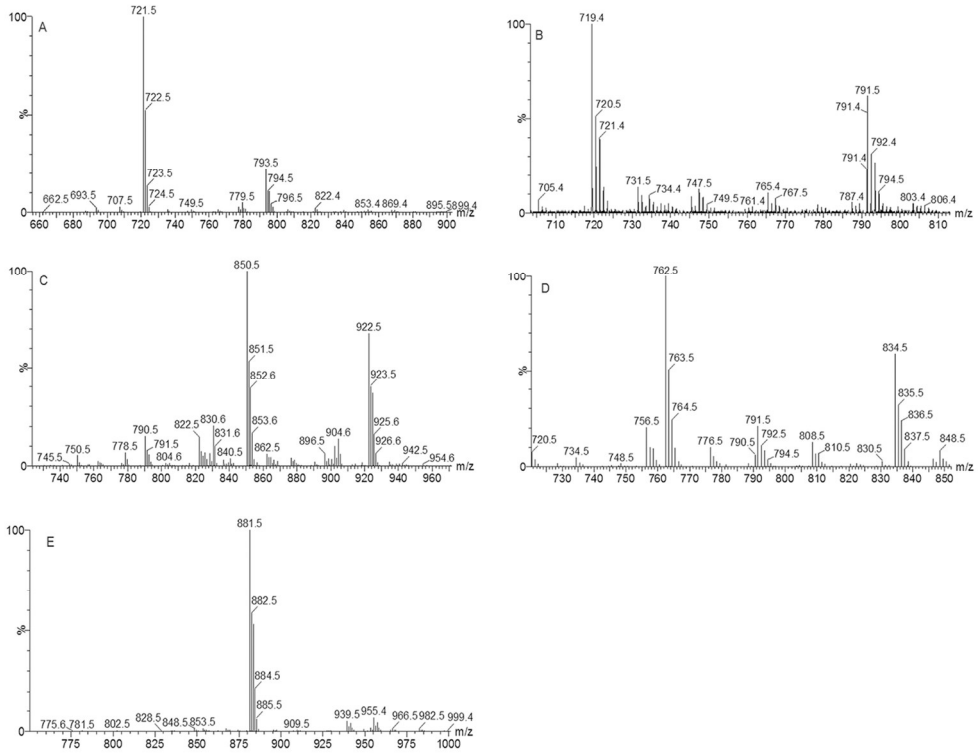

126x106mm (300 x 300 DPI)

Figure 4

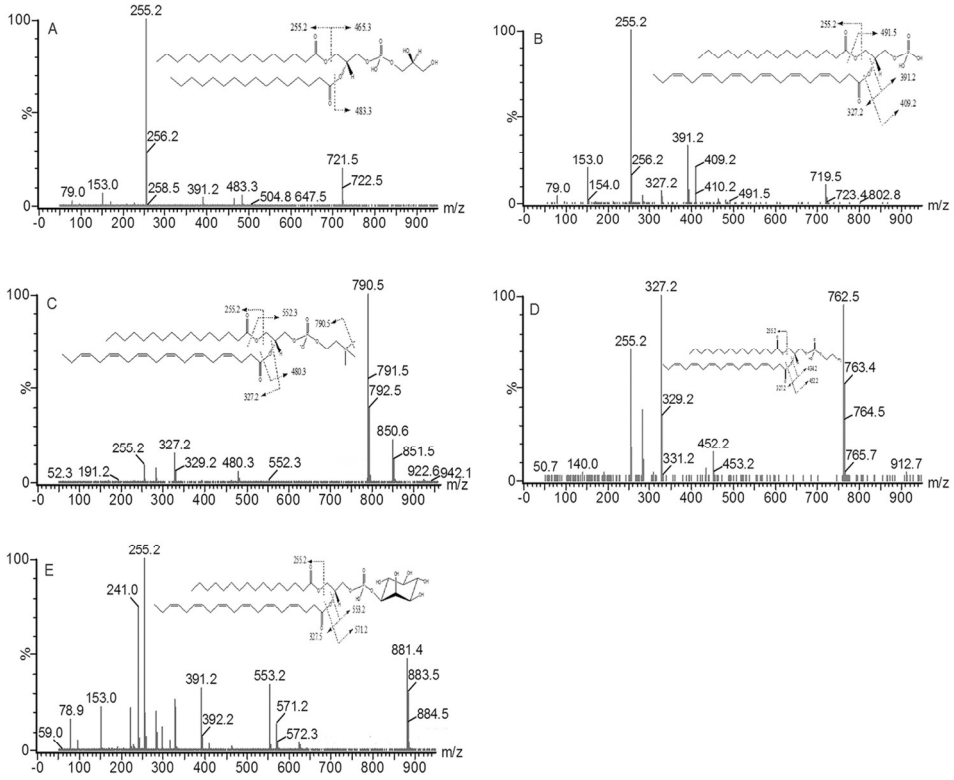

132x116mm (300 x 300 DPI)

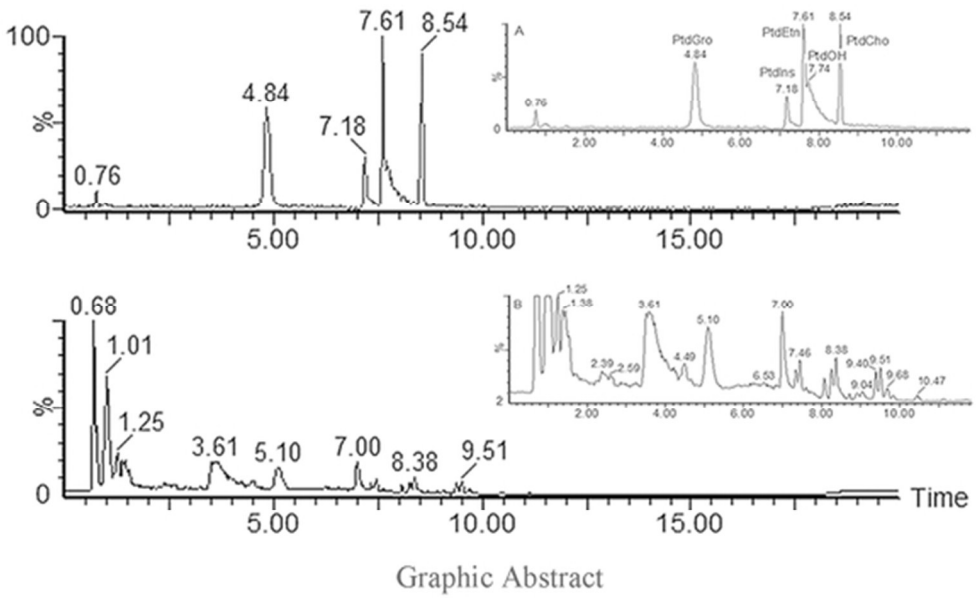

Graphic Abstract

49x35mm (300 x 300 DPI)